Optimizing Navigator Flip Angle for Free-Breathing Fat-Fraction and R2* Quantification of the Liver

James H. Holmes[1], Diego Hernando[2], Yuji Iwadate[3], Ann Shimakawa[4], Gavin Hamilton[5], Utaroh Motosugi[2], and Scott B Reeder[2,6]

[1]*Global MR Applications and Workflow, GE Healthcare, Madison, WI, United States,* [2]*Radiology, Univeristy of Wisconsin-Madison, Madison, WI, United States,* [3]*Global MR Applications and Workflow, GE Healthcare, Hino, Tokyo, Japan,* [4]*Global MR Applications and Workflow, GE Healthcare, Menlo Park, CA, United States,* [5]*Radiology, University of California San Diego, San Diego, CA, United States,* [6]*Medical Physics, University of Wisconsin-Madison, Madison, WI, United States*

Introduction: Chemical shift encoded (CSE) techniques, using multi-echo spoiled gradient-echo (SPGR) sequences can be used for accurate proton density fat-fraction (PDFF) and R_2* quantification in the liver [1]. In order to obtain accurate measurement of liver PDFF, multiple confounding factors need to be addressed, including T_1 bias resulting from different T_1 values of fat and water [2,3]. Typically, "T_1-independent" acquisitions are performed by using low flip-angles resulting, in proton-density contrast [2]. These techniques are currently acquired in a single ~20s breath-hold. However, breath-holds of any duration are challenging for some patients including children, approximately 10% of whom have fatty liver disease [4]. Motion compensation would significantly aid in the clinical utility of these methods. Navigators have been used to improve motion robustness [5], however, one challenge of the navigated methods is potential for changes in the steady state of the magnetization in the imaging volume (ie: introducing T_1 bias) as well as the need for robust edge detection for motion tracking. A trade-off exists between high signal for navigator motion detection and maintaining high steady-state signal for imaging (Fig. 1). ***In this work***, we optimize the navigator flip angle to minimize T_1-related fat quantification errors while maximizing signal for motion tracking.

Figure 1. *A) Axial navigated IDEAL PDFF maps showing uniform signal in the liver with a navigator flip angle of 10° and PDFF of 20% at the site of the navigator excitation. B) Image acquired using a very high 90° navigator flip angle reporting a PDFF of 69% at the site of the navigator (red arrow).*

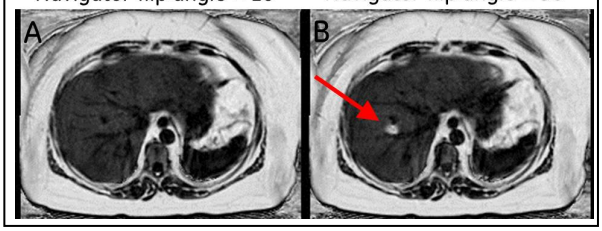

Table 1. *Target and measured fat fractions and T_1 times.*

PDFF Target	PDFF (IDEAL-IQ)	PDFF (spectroscopy)	Fat T1 (spectroscopy)	Water T1 (spectroscopy)
0	1.2	0.9		1075.6ms
10	7.8	8.7	345.0ms	1137.4ms
30	29.8	27.1	347.2ms	1126.7ms
50	48.2	49.1	367.8ms	1168.0ms

Methods: Imaging was performed on a 3T clinical MRI (MR750, GE Healthcare, Waukesha, WI) using an 8-channel receive array coil (Invivo Corporation, Orlando, FL). Navigated multi-echo CSE (IDEAL IQ) acquisition parameters included: 40×40×25.6 cm FOV, 160 ×160 × 32 acquired matrix, 6 echoes over 2 separate shots, +/-142.8 BW, 3° imaging flip angle, and 200ms between navigators. Navigators were acquired using a cylindrical excitation and readout over a length of 20 cm and diameter of 20 mm. The chemical shift due to temperature was accounted for in the IDEAL reconstructions [6]. Individual PDFF phantoms were built using specific concentrations of peanut oil with a mixture of water, agar, NaCl, CuSO4 and surfactant [7]. Separate R_2* phantoms were built using Feraheme (iron) rather than oil (Table 2). Respiratory motion was simulated using a linear sinusoid with 30mm/s peak velocity, 30mm travel, and 0.4s dwell time. The PDFF and T_1's of fat and water were measured in each phantom using a multi-TR/TE single-voxel spectroscopy acquisition [8].

Table 2. *Feraheme concentration vs. R_2* in iron phantoms.*

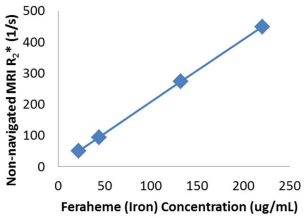

Results: Images in a volunteer demonstrate good PDFF map quality during free breathing. However, at a high navigator flip angle of 90°, the local PDFF was over estimated (Fig. 1, arrow). Plots of the phantom signal in the navigator show increased signal with higher flip angles (Fig. 2a). The PDFF measured in the navigated images were in good agreement with the theoretical and spectroscopy values at navigator flip angles of 10 degrees and lower (Table 1, Fig. 2b). However as the navigator flip angle was increased to 30 degrees and above, significant signal attenuation was observed in the source images and deviations were observed at the site of navigator excitation. This effect was greater in higher fat content phantoms. Separate measurements in phantoms made with reduced $CuSO_4$ concentrations resulted in longer water T_1's and showed an even greater sensitivity to navigator flip angle. Although the attainable navigator signal was much higher at large flip angles, this introduced significant signal loss in the individual echo images acquired for the IDEAL IQ processing. The R_2* values were unaffected by the navigator and were very consistent (Fig. 2c).

Figure 2. *Measured fat-fraction as a function of navigator flip angle in 0% fat-fraction phantom showing increased bias with larger navigator flip angles a). Signal measured in the navigator profile during the imaging acquisition as a function of navigator flip angle b).*

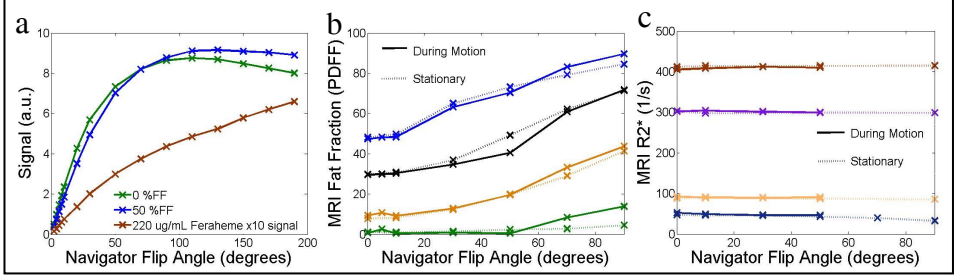

Conclusions: Navigated IDEAL enabled measurement of PDFF and R_2* values in moving phantoms that were in good agreement with stationary imaging and spectroscopy measurements so long as the navigator flip angle was limited to 10°. The navigator pulse width of 6 ms resulted in sufficient time for incomplete excitation due to rapid relaxation rates. Although at higher navigator flip angles there was greater signal for navigator motion detection, a bias was observed toward higher PDFF at the navigator location due to greater signal saturation of the longer T_1 species (water). The T_1 of water and fat observed in the phantoms were in agreement with previous in vivo liver measurements [8].

References: [1] Yu et al. MRM 2008 ;60 :112-1134. [2] Liu et al. MRM 2007;58:354–364. [3] Bydder et al MRI 2008;26:347-359. [4] Schwimmer et al. Pediatrics 2006 ;118 :1388-1393.[5] Ehman Radiology 1989 ;173 :255-263 [6] Hernando et al. MRM 2013;early view [7] Hines et al. JMRI 2009 ;30 :1215-1222. [8] Hamilton et al. ISMRM 2013, A1517.

Acknowledgements: NIH (R01 DK083380, R01 DK088925) and the WARF Accelerator Program.